

# LangNavBench: Evaluation of Natural Language Understanding in Semantic Navigation

Sonia Raychaudhuri<sup>1</sup>, Enrico Cancelli<sup>2</sup>, Tommaso Campari<sup>3</sup>,  
Lamberto Ballan<sup>2</sup>, Manolis Savva<sup>1</sup>, Angel X. Chang<sup>1,4</sup>

<sup>1</sup>Simon Fraser University, <sup>2</sup>University of Padova,

<sup>3</sup>Fondazione Bruno Kessler (FBK), <sup>4</sup>Alberta Machine Intelligence Institute (Amii)

<https://github.com/3dlg-hcvc/langmonmap>

## Abstract

Recent progress in large vision-language models has driven improvements in language-based semantic navigation, where an embodied agent must reach a target object described in natural language. Despite these advances, we still lack a clear, language-focused benchmark for testing how well such agents ground the words in their instructions. We address this gap with LangNav, an open-set dataset specifically created to test an agent’s ability to locate objects described at different levels of detail, from broad category names to fine attributes and object-object relations. Every description in LangNav was manually checked, yielding a lower error rate than existing lifelong- and semantic-navigation datasets. On top of LangNav we build LangNavBench, a benchmark that measures how well current semantic-navigation methods understand and act on these descriptions while moving toward their targets. LangNavBench allows us to systematically compare models on their handling of attributes, spatial and relational cues, and category hierarchies, offering the first thorough, language-centric evaluation of embodied navigation systems. We also present Multi-Layered Feature Map (MLFM), a method that builds a queryable multi-layered semantic map, particularly effective when dealing with small objects or instructions involving spatial relations. MLFM outperforms state-of-the-art mapping-based navigation baselines on the LangNav dataset.

## 1 Introduction

Semantic navigation is a rapidly growing sub-field in embodied AI [11] where an agent is tasked with navigating to a target object described using either an object category [1, 3, 46], image [22] or natural language descriptions [26, 36]. Each of these target specifications poses unique challenges, especially natural language, which is inherently ambiguous and context-dependent. In this paper we focus on natural language driven semantic navigation. To construct datasets with descriptions, prior works [21] use large vision-language models (VLM) to extract attributes about an object from an image, followed by merging the attributes into coherent sentences using a large language model (LLM). However, VLMs often contain hallucination errors [27] in extracting object attributes, especially in cluttered or out-of-distribution scenes. Such hallucinated attributes introduce significant noise, biasing both agent learning and fair evaluation. Moreover, despite considerable progress in improving semantic navigation task performance, very little focus has been given to how well the agents understand and act on different natural language cues which are used to specify the goal, such as references to object attributes and relationships. To address these gaps, we introduce a benchmark, LangNavBench, and systematically study the state-of-the-art methods with a focus on various natural language understanding components. We use the scenes, objects and ground-truth attributes from the Habitat Synthetic Scenes Dataset (HSSD) [20] to avoid errors from VLMs.



Figure 1: **LangNavBench** provides a means to evaluate natural language understanding in semantic navigation methods by introducing LangNav dataset that not only uses natural language to describe goal objects but also stores linguistic annotations for each description. (Left) a single object can be described using descriptions with varying specificity ranging from no attribute to using multiple attributes. (Right) semantic navigation gets harder with increasing number of attributes in the description, since it requires the agent to navigate to a very specific object instance.

Prior work in vision-and-language navigation (VLN) instructs the agent with a *full route*—for example, “leave the bedroom, turn left, pass the painting, and stop at the sofa” [2, 23, 35]. Because these descriptions are crowdsourced, they rarely contain hallucinated attributes, yet the task couples object grounding with the added challenge of parsing route directives.

In everyday settings, however, people rarely spell out an entire path; they simply name the goal—“bring me the blue mug on the bedside table.” Goal-only language is therefore both *natural* and *challenging*: the agent must explore unseen space, decide when it has found the right object, and remember what it has already observed. Sequential tasks such as Multi-Object Navigation (MultiON) [38, 34, 21] capture part of this difficulty by revealing each target only after the previous one is reached, but they supply limited linguistic variety.

Our LangNavBench extends this idea. Each episode presents three goals in succession, each described in natural language that may include colour, size, material, or support relations. Success therefore hinges on two abilities: (i) building a semantic map memory while exploring, and (ii) querying that memory to reason about objects whose descriptions vary in granularity. LangNavBench focuses on goal-specific language instructions and offers a testbed for systematically evaluating these two aspects in map-based navigation methods.

In summary, our contributions are threefold: (i) *LangNavBench*: a benchmark to evaluate semantic navigation agents on their ability to understand natural language based on various linguistic cues (color, size, texture, state, number, material, lexical modifiers, and support relations); (ii) *LangNav*: an open-set multi-object navigation evaluation dataset with episodes containing natural language descriptions for goals with varying amount of specificity and language cues that exist in the description; (iii) *MLFM*: a multi-layer semantic-mapping approach that preserves intricate features about objects in the environment without the cost of full 3D mapping and achieves improved performance over current SOTA mapping-based semantic navigation baselines on the LangNav dataset.

## 2 Related Work

**Semantic navigation.** In embodied AI, one of the basic semantic navigation tasks is the Object Navigation (ObjectNav), where an agent is required to navigate to an object specified by its category. While earlier benchmarks [1, 3] have used a closed set of object categories, HM3D-OVON [46] introduces a benchmark containing open-vocabulary categories to describe the goal. Multi-Object Navigation (MultiON) [38] extends this single object navigation to multi-object setting where multiple objects are made available to the agent in sequence. MultiON requires the agent to remember objects observed in the past so as to come back to it if needed, for efficiency. Another type of semantic

navigation is the Instance-Nav [22], where the agent is given an image of the goal object to find. While this task has its own challenges with respect to finding a specific object instance observed from a specific view angle, it does not reflect real-world scenarios where it is more likely for someone to describe an object of interest in words. A more natural semantic navigation is where the goal object is described using natural language, a task called language-based InstanceNavlanguage description [26, 36]. GOAT-Bench [21] has been recently introduced to provide a benchmark on multi-modal navigation, where they combine different modalities (object category, image and language) to specify the goals, and the agent is tasked with finding multiple goals in sequence. In this paper we focus on a single modality, language, to specify goals in a multi-object navigation task.

**Semantic maps.** A widely used representation in semantic navigation is a semantic map that serves as a memory of observations that the agent has made throughout its navigation. It has been shown to improve efficiency in the longer-horizon MultiON task [21] by remembering objects of importance. While some works [8, 14, 48] store explicit information such as object category in the map, more recent methods store implicit features in the map [17, 13, 9], enabling open-vocabulary memory representation. These features are often extracted from a large VLM such as CLIP [33]. VLMs [17] use pixel-level embeddings from LSeg [24], while VLFM [45] uses BLIP-2 [25] image features to build a 2D top-down map and compute semantic frontiers to explore the environment while performing navigation. Others build 3D maps [47, 15] to preserve every geometric detail about the objects, which allows better reasoning, but are very costly to build and maintain, especially in long-horizon tasks. In this work, we propose a multi-layer map that serves as a middle-ground between a 2D and a 3D map and contains stacked layers of 2D maps, providing more granularity and flexibility than a 2D map but avoids the cost of a 3D map.

**Evaluation benchmarks and datasets.** Evaluating AI models against natural language understanding has gained a lot of interest in 3D scene understanding and grounding. OpenLex3D [18] proposes a benchmark that evaluates open-vocabulary scene representation methods by introducing new label annotations, such as synonyms, depictions, visual similarity, and clutter, in existing scene datasets. Eval3D [12] proposes an evaluation tool to evaluate 3D generative models to assess their geometric and semantic consistencies. Agentbench [30] introduces a test bed to systematically evaluate LLMs acting as agents on their reasoning capabilities. ViGiL3D [37] introduces a dataset for evaluating visual grounding methods with respect to a diverse set of language patterns, such as object attributes, relationships between objects, target references, etc. Similarly to ViGiL3D, we introduce a benchmark to evaluate semantic navigation methods with respect to object attributes and relationships extracted from the language descriptions that specify goal objects in our dataset.

### 3 LangNavBench

#### 3.1 Benchmark design

Our benchmark offers a thorough assessment of semantic-navigation methods by measuring how well they ground linguistic cues — object attributes and object relationships while traveling to each goal. We frame the problem as a *multi-object semantic-navigation* task in which the agent must reach several goals sequentially. Each goal is specified by a natural-language description whose specificity ranges from a coarse category (e.g., ‘candle’) to a uniquely defined instance (e.g., ‘the red short pillar candle on the night-stand’). If the description is coarse, multiple valid targets may be present and reaching any one of them counts as success; when the description is fine-grained, it typically refers to a single object, making the episode harder because the agent must disambiguate that specific instance.

Following ViGiL3D [37], we evaluate grounding accuracy with respect to eight linguistic features: • **Color**—a colour adjective in the description, e.g. ‘the *brown* chair’. • **Size**—an explicit size cue, e.g. ‘the *small* candle’. • **Texture**—a surface pattern or finish, e.g. ‘*knitted* bath mat’. • **State**—a transient state that could change, e.g. ‘*illuminated* makeup mirror’. • **Number**—a numeral in the description, e.g. ‘the cabinet with *two* doors’. • **Material**—the substance an object is made of, e.g. ‘*wooden* shoe rack’. • **Modifier**—any other adjectival qualifier, e.g. ‘the *easy* chair’. • **Support relationship**—an explicit support relation, e.g. ‘the potted plant *on* the console table’.

### 3.2 Dataset

To implement LangNavBench, we introduce a new dataset, *LangNav*, where the goal objects are specified using language descriptions. Each episode contains *three* goals, disclosed to the agent one at a time rather than all at once. Revealing every target at the start would let the agent approach each object the moment it first appears, undermining our aim of testing how well it stores and reuses information gathered during exploration. The descriptions can detail an object with various amounts of specificity, for example ‘Go to the couch’ vs ‘Go to the black couch’ vs ‘Go to the black three piece L-shaped sectional couch’. This allows us to evaluate the agent’s capability to identify objects specified without any attribute as well as those specified by one or more attributes.

**Why the need for a new dataset?** There are a few datasets (Tab. 1) available in the community to evaluate ObjectNav [1, 3]. The most close to ours is Goat-Bench [21] which introduced a multi-object navigation dataset that combines ObjectNav and InstanceNav goal descriptions. Their pipeline derives object attributes by prompting a pretrained BLIP-2 model, and this reliance on automatic extraction introduces noticeable noise in the captions. Typical issues include (i) *partial matches*, where the instruction fits the target only in part; (ii) *hallucinations*, where attributes mentioned in the text are absent from the scene; and (iii) *mesh artefacts*, where incomplete geometry in HM3D-Sem hides the object, rendering the description misleading (see supplementary for qualitative results). We mitigated these errors by first using scenes and objects from the high-quality synthetic HSSD dataset. The scenes in HSSD are synthetic, hence free of mesh-related issues. The dataset also provides ground-truth categories and attributes for every object; we pass this structured metadata to GPT to obtain fluent natural-language instructions that remain anchored to the ground truth. All generated sentences are then manually reviewed and, where necessary, corrected to eliminate any residual LLM errors. Finally, we tag each instruction with the linguistic cues used in our benchmark (colour, size, material, state, and so on) and release these annotations with the dataset—information that no previous semantic-navigation corpus offers.

Table 1: **Comparison with prior datasets.** LangNav provides ObjectNav as well as language-based InstanceNav goals, with additional linguistic features for the goal descriptions.

Datasets	Task	ObjectNav goals	InstanceNav language goals	Open vocabulary	Linguistic features	No significant description errors
OVMM[44]	Manipulation	✓	×	✓	×	-
ObjectNav[3, 42]	Object nav	×	×	×	×	-
HM3D-OVON[46]	Object nav	✓	×	✓	×	-
MultiON[38, 34]	Multi-object nav	✓	×	×	×	-
OneMap[6]	Object nav, Multi-object nav	✓	×	×	×	-
Goat-Bench[21]	Multi-(object+instance) nav	✓	✓	✓	×	×
<i>LangNav</i>	Multi-(object+instance) nav	✓	✓	✓	✓	✓

**Episode generation.** We use the high-quality synthetic 3D scenes from HSSD [20] to generate our episodes. We select goals from the objects available in HSSD. For each episode we first draw a random navigable start pose for the agent, then choose an object category that satisfies the following constraints: (i) at least one navigable viewpoint lies within 1.5 m of the object; (ii) the start pose and all three goals are on the same floor; (iii) every goal is reachable from the start pose; (iv) each goal is at least 2 m from the start pose; (v) the geodesic-to-Euclidean distance ratio from the start pose to each goal exceeds 1, ensuring non-trivial navigation; (vi) the geodesic distance from the start pose to the first goal is at least 2.5 m. For each goal, we also store ‘viewpoints’ or navigable positions around the goal object, such that navigating near to any of those will be considered successful (see supplementary).

**Language descriptions.** We convert the ground-truth attributes and support relations available in HSSD into fluent object descriptions with GPT-4 [32]. The model is prompted with a short instruction plus in-context examples [5, 28, 40]: “You are given a list of attributes for an object. Using them, form a coherent description such that a human can find the object in a scene.”

Each description is then wrapped in a standard navigation template (e.g., Find ..., Go to ...) to create the final instruction. All sentences are manually reviewed and, where needed, edited to correct residual LLM errors. Finally, following the procedure of ViGiL3D [37], we use GPT-4 to

tag every instruction with the linguistic features employed in our benchmark—colour, size, material, state, and so on—and release these annotations with the dataset.

**Statistics.** We provide two splits for our dataset, validation and test with distinct set of target objects and distinct scenes. The validation split contains 832 episodes, each with three goals, totaling to 2496 goal descriptions spanning across 20 scenes, whereas the test split contains 750 episodes, each with three goals, totaling to 2250 goal descriptions spanning across 15 scenes. Tab. 2 shows the dataset statistics.

Table 2: **Dataset statistics.** LangNav contains val and test splits, each with distinct sets of scenes and goal object categories. The goal descriptions might contain one or more linguistic features.

	Validation	Test	Overall
scenes	20	15	35
episodes	832	750	1582
distinct object categories	19	12	31
distinct object instances	160	91	251
goal descriptions	2496	2250	4746
descriptions with attributes/relationships	1659	1874	3533
total linguistic features	2534	3108	5642
unique linguistic feature values	136	92	228

### 3.3 Evaluation

We evaluate how the semantic navigation methods perform across the various aspects of the language descriptions. We use the standard navigation metrics, the success rate (*SR*) and the success weighted by inverse Path Length (*SPL*) [1] to measure whether the agent can reach a target object successfully and how well the agent trajectory matches the shortest path to the target respectively. More specifically, we report *SR* and *SPL* against each of the linguistic features described in Sec. 3.1. We follow the task setup from Goat-Bench, where the agent is given a time budget of 500 steps to navigate to each goal in a sequence of multiple goals, and the episode continues even when the agent fails to navigate to one goal.

## 4 Method

We present MLFM, which incrementally builds a multi-layer semantic map. At each step the goal description is embedded and treated as a convolutional text-kernel that is slid over the map layers, producing a similarity heat-map that ranks every cell. For composite queries with support relations (e.g., “candle on the night-stand”) the kernel contains separate embeddings for the supported and supporting objects and is evaluated across height bands. When a cell in the map is marked as a possible target location, an open-vocabulary detector checks the prediction, and the goal is accepted only if both sources agree i.e., via consensus filtering [6]. An A\* planner is used to compute the agent’s actions.

### 4.1 Mapping

#### Map building.

The map must capture vertical context without incurring the cubic memory cost of a full 3-D voxel grid. Flattening everything into a single 2-D plane is usually an effective solution, but it merges features from stacked objects—small items vanish beneath larger ones—and discards the height cues needed for reasoning about support relations. We therefore adopt a *multi-layer* top-down map that stores only a handful of horizontal slices: granular enough to separate objects at different heights, yet linear in memory and update cost.

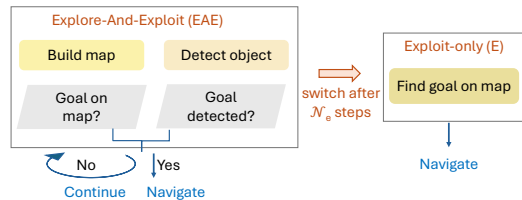


Figure 2: **MLFM** builds a multi-layer feature map, verifies candidates with an object detector, and navigates in two stages, EAE-E once the map is deemed reliable.



To this end, we build a multi-layer feature map,  $\mathcal{M} \in \mathbb{R}^{L \times h \times w \times f_d}$  where  $L$  is the number of layers, each containing a 2D top-down map  $m \in \mathbb{R}^{h \times w \times f_d}$  and  $f_d$  is the feature dimension stored at each map cell.  $h$  and  $w$  correspond to the  $(X \times Y)$  space of the physical environment, while  $L$  corresponds to its discretized height dimension  $Z$ . Fig. 3 presents a schematic of the map building process. Given the RGB observation  $I_t \in \mathbb{R}^{H \times W \times 3}$  at each step  $t$ , we extract patch-wise features  $Fp_t \in \mathbb{R}^{H \times W \times n_p \times f_d}$  using CLIP image encoder from SED [41]. We rely on a CLIP-based vision-language model to store features embedded in a joint image-text space, so that the map can be queried with natural-language descriptions. Here  $n_p$  is the number of patches. Using the depth observation  $D_t \in \mathbb{R}^{H \times W}$  and the camera intrinsics, we then project the features  $Fp_t$  onto a 3D point-cloud. Next we project the 3D points onto the 2D plane. For each point  $p_i$  in the point-cloud at the 3D location  $(x_i, y_i, z_i)$ , we find the appropriate layer using the height  $z_i$  of the point in the point-cloud, such that:  $l_i = \lfloor \frac{h_i}{\Delta h} \rfloor$ , where  $l_i$  is the layer index and  $\Delta h$  denotes the height range of each layer.

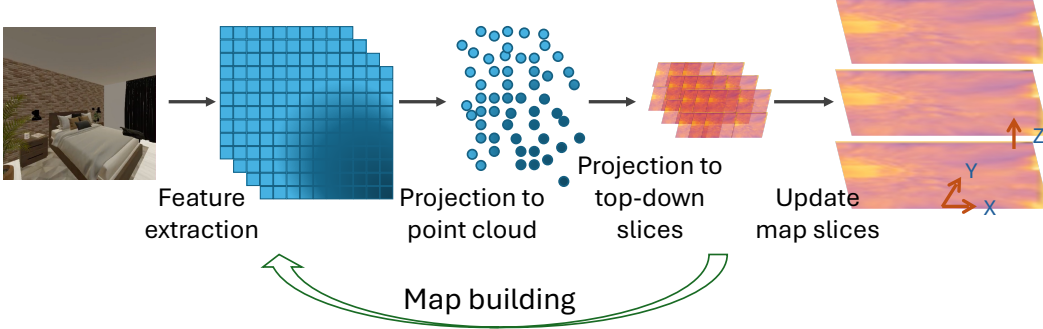


Figure 3: We build a multi-layer feature map where each layer contains a 2D top-down map.

**Map querying (text-as-a-kernel).** To locate the target object on the map  $\mathcal{M}_t$  at time  $t$ , we first build a similarity map  $S_t \in \mathbb{R}^{L \times h \times w}$ . For each cell  $c = (l, x, y)$  we compute the cosine score  $s = \frac{\mathcal{F}_t \cdot \mathcal{Z}}{\|\mathcal{F}_t\| \|\mathcal{Z}\|}$ , where  $\mathcal{F}_t$  is the image feature stored in the map and  $\mathcal{Z} = f(g) \in \mathbb{R}^{1 \times f_d}$  is the text embedding of the goal description  $g$  obtained with the encoder  $f$ . The cell with the highest score is treated as the predicted goal location. For instructions that contain relationships between objects (e.g., “find the candle on the night-stand”), we embed the objects  $g_1$  and  $g_2$  separately, yielding  $\mathcal{Z} = f(g_1, g_2) \in \mathbb{R}^{2 \times f_d}$ . For support relations, we apply this two-vector “text kernel” across layers so that matches in a higher layer  $l_j$  are evaluated with respect to potential supports in the immediately lower layer  $l_{j-1}$ , mirroring their physical arrangement. Note that text-as-a-kernel has been found effective when used in convolution networks in prior works [4, 31]. The feature map  $\mathcal{M}$  is preserved throughout the episode to allow cumulative search, whereas the similarity map  $S$  is reset after each goal is completed.

## 4.2 Navigation pipeline

**Two phase navigation (EAE-E).** At the beginning of an episode the map is still sparse and, because it stores *features* rather than explicit class labels, its cosine scores can be noisy. An open-vocabulary detector, such as YOLO-World [10], on the other hand, yields high-precision category predictions whenever the object is in view. Hence, early on the detector is the more reliable signal, while the map serves mainly to propose candidate locations that must later be verified by the detector; as exploration continues and the map densifies, trust gradually shifts toward the map. Following this idea we therefore divide navigation into two phases: (i) **Explore-And-Exploit (EAE)**. For the first  $\mathcal{N}_e$  steps a location is accepted as the goal only if *both* the similarity map  $S$  and the detector agree. Upon agreement the agent moves to that cell via the path planner; otherwise it resumes exploration. (ii) **Exploit-only (E)**. After  $\mathcal{N}_e$  steps—within the total budget  $\mathcal{N}$ —the agent relies solely on the map: it selects the cell with the highest cosine similarity to the goal description and heads directly to it.

## 5 Experiments

In this section, we present a comprehensive evaluation of state-of-the-art semantic navigation methods on our LangNav dataset and compare with our zero-shot method, MLFM (see supplementary for Goat-Bench results).

## 5.1 Implementation

For all the zero-shot baselines, we use an A\* [16, 6] planner. The agent takes as inputs egocentric RGB-D images as well as GPS and compass readings relative to the starting pose in the episode. It also has access to the language instruction describing the current goal  $g_i$  at any given time step. The action space is composed of four actions: *move forward* by 25 cm, *turn left* by 30°, *turn right* by 30°, and *found*. An episode is considered successful if the agent generates a *found* action within 1.5 meters of the goal. We use SED [41] patch features to build the multi-layer map and Yolo-World as an object detector in MLFM. Our map has three layers and each 2D grid cell maps to 6 cm in the physical space. Using 1×A40 GPU, it takes ∼8 hours for evaluating our method on the full test split.

## 5.2 Baselines

We focus on understanding how an explicit memory—in our case, a semantic map—helps agents solve the tasks in LangNav, especially when the goal descriptions vary in linguistic attributes. Accordingly, we compare MLFM with state-of-the-art *mapping-based* navigation methods: VLMaps [17] and VLFM [45], which achieve strong performance on ObjectNav with 2D semantic maps, and OneMap [6] and MOPA [34], which proved effective on the MultiON task. For VLMaps and VLFM we extend the original ObjectNav code to the multi-goal setting by running their policy sequentially for each target while preserving the feature map across goals, so that every method benefits from the same accumulated memory within an episode.

**VLMaps** [17] store LSeg [24] pixel-level embeddings in a 2D top-down grid map, along with their 3D location. They average the pixel embeddings when multiple pixels are projected onto the same grid and also across multiple views.

**VLFM** [45] builds a 2D value map that stores BLIP-2 [25] similarity scores of the observed images and object category, and uses it to semantically explore the environment. It achieves SOTA performance in the ObjectNav task.

**MOPA** [34] iteratively builds a 2D category map after detecting objects in the frame, randomly explores the environment and navigates to the goal once found. We replace their PointNav [39] with the A\* planner for fair comparison.

**OneMap** [6] builds a 2D feature map with SED [41] patch features by using a confidence-based fusion mechanism. They employ an open-set object detector YOLO-World [10] along with the map to identify the target and use an A\* planner to navigate.

We also have two additional baselines, **VLFM-v2** and **OneMap-v2**, where we adapt the two phase-navigation EAE-E (Sec. 4.2), explore-and-exploit (EAE) followed by exploit-only (E) phases, for the two baselines, VLFM and OneMap.

## 5.3 Results and discussion

Tab. 3 shows that on LangNav, MLFM significantly outperforms the semantic navigation SOTA methods on the overall SR and SPL metrics. MLFM achieves +30.3% increase in SR and +11.5% increase in SPL over OneMap and +40.6% increase in SR and +15.9% increase in SPL over VLFM. The poor performance in VLFM is due to the fact that it relies only on the built map, even during the initial stages of navigation when the map may not contain the target object. This is evident from the improved performance of VLFM-v2 (+21.8% and +8.7% increase in SR and SPL respectively) over the vanilla VLFM, where we adapt the two-phase navigation. We observe a similar trend in OneMap, where OneMap-v2 achieves +26.1% and +9.7% increase in SR and SPL respectively. This demonstrates that *our two-phase navigation (EAE-E) approach is extremely effective* when dealing with long-horizon tasks.

Additionally, MLFM outperforms other 2D map-based methods on the ‘support’ category (+5.2% gain from OneMap-v2) to indicate that *our text-as-a-kernel querying is very effective in descriptions containing support relations*. It confirms our hypothesis that using text as a kernel on the features stored across multiple layers in the map enables us to leverage the support structure better.

Moreover, MLFM outperforms the 2D map-based methods on descriptions without attributes and with color, number, material and modifier attributes by large margins (+8.8%, +11.6%, +7.2%, +21.3% and +6.8% gains over OneMap-v2 respectively). This demonstrates that *our layered map representation*

*captures image features better than a 2D map*, where the projected features are aggregated on a single layer, making it hard to distinguish intricate details about the objects.

However, MLFM fails to identify texture (0% SR) of objects. This is mostly the limitation of the feature extractor used in MLFM, as confirmed in the ablation Sec. 6.1. MLFM also fell short of OneMap-v2 on descriptions with the state attribute. To understand the reason behind this, we perform failure analysis in Sec. 5.4.

Note that we ran each of OneMap-v2, VLFM-v2 and MLFM five times with random seeds and observe a standard deviation of  $\pm 2.5$  for each. In the tables, we report the mean performance over five runs.

Table 3: **LangNav performance.** MLFM outperforms the baselines on the overall SR and SPL. It also achieves highest SR on descriptions without attributes (‘no’) and on the ‘color’, ‘number’, ‘material’ and ‘modifier’ attributes as well as on the ‘support’ relations.

Methods	SR $\uparrow$	SPL $\uparrow$	SR $\uparrow$								
			no	color	size	texture	number	material	state	modifier	support
VLMs	2.0	0.5	1.1	0.0	0.0	0.0	0.0	0.0	0.0	0.1	0.0
VLFM	3.0	1.0	2.4	0.0	0.0	0.0	0.0	0.0	0.0	1.0	0.0
MOPA	7.9	2.4	2.8	1.6	1.6	0.0	0.0	0.0	0.0	3.2	1.9
OneMap	13.3	5.4	3.7	2.7	6.7	0.0	0.0	0.0	0.0	6.7	9.7
VLFM-v2	24.8	9.7	28.2	11.5	33.3	0.0	7.1	43.1	28.6	17.7	12.9
OneMap-v2	39.4	15.1	29.1	26.9	<b>41.7</b>	0.0	7.1	0.0	<b>57.1</b>	21.1	22.1
MLFM (Ours)	<b>43.6</b>	<b>16.9</b>	<b>37.9</b>	<b>38.5</b>	<b>41.7</b>	0.0	<b>14.3</b>	<b>64.4</b>	14.3	<b>27.9</b>	<b>27.3</b>

## 5.4 Failure analysis

**MLFM vs OneMap-v2.** To understand why OneMap-v2 performs better than MLFM for descriptions with state attribute, we look at the error cases in Tab. 4. We report the percentage of times the agent makes a wrong detection, identifies the wrong goal on the map or runs out of time. First, there are more wrong detection cases than wrong goal on map for both the methods. This indicates that the performance could be improved by using a better object detector, an observation also confirmed in our ablation Sec. 6.2. Second, MLFM and OneMap-v2 have same wrong goal on map percentage, indicating that this error type is not due to using multi-layer map instead of 2D map. Moreover, an ablation in Sec. 6.1 indicates that the performance could be improved by using image-level features instead of patch-level features.

**Overall MLFM failure.** Performing a similar failure analysis on the overall performance of MLFM, we observe that 31.7% of the error cases are due to wrong detection and 17.0% is due to wrong goal identification on map. The rest 48.3% is due to the agent running out of time budget while exploring and 3% is where the agent identifies the goal but fails to reach it on time.

Table 4: **Failure analysis** for MLFM vs. OneMap-v2.

Methods	Wrong detection	Wrong goal on map	OOT
MLFM	71.4	14.3	14.3
OneMap-v2	28.6	14.3	57.1

## 6 Ablations

### 6.1 Ablation with feature extractors

We gauge the effect of different open-vocabulary feature extractors within MLFM to determine which image features yield the most informative multi-layer map. Table 5 compares *image-level* and *patch-level* embeddings.

Patch features are clearly superior: compared with their image-level counterparts (rows 1–2 vs. 3–4), SED-CLIP and BLIP-2 patches raise SR by +11.8% and +8.0%, and SPL by +4.7% and +0.5%, respectively. The explanation is twofold. First, when we store the same global feature vector in every layer (CLIP or BLIP image-level), the map gains no additional information. Second, SED [41] and BLIP-2 patch embeddings preserve spatial alignment as well as finer image–text correspondence.



The benefit is most pronounced (rows 2 vs 4) for support relations (+6.4%) and for colour, size, material, and modifier cues (+26.9%, +25.0%, +16.3%, +3.1%, respectively), and even for descriptions without explicit attributes (+1.0%). Conversely, image-level features edge out patches on *number* and *state* attributes (rows 2 vs. 4), suggesting that a holistic view occasionally helps when counting instances or detecting object states. BLIP-2 outperforms CLIP on texture and number recognition (row 4 vs. 3), confirming its stronger vision–language alignment for such properties.

Finally, pixel-level embeddings from LSeg perform worst overall (row 5), indicating that overly fine-grained features hinder object-level reasoning and dilute the broader context captured by patch- or image-level representations.

Table 5: **Ablations.** Patch-level features outperforms image-level features followed by pixel-level features in the overall SR and SPL. Image-level features, however, perform better when there are no attributes in the descriptions or the ones with state attribute. Grounding-dino outperforms Yolo-World in size and state attributes and descriptions with no attributes.

Object detector	Features	Type	SR↑	SPL↑	SR↑								
					no	color	size	texture	number	material	state	modifier	support
1 YOLO-World [10]	SED [41]	patch	<b>43.6</b>	<b>16.9</b>	37.9	<b>38.5</b>	41.7	0.0	14.3	<b>64.4</b>	14.3	<b>27.9</b>	<b>27.3</b>
2	BLIP-2 [25]	patch	40.5	15.4	35.9	34.6	41.7	<b>20.0</b>	14.3	16.3	14.3	24.9	26.0
3	CLIP [33]	image	31.8	12.2	31.1	11.5	8.3	0.0	0.0	0.0	28.6	17.1	17.7
4	BLIP-2 [25]	image	32.5	14.9	34.9	7.7	16.7	<b>20.0</b>	<b>21.4</b>	0.0	28.6	21.8	19.6
5	LSeg [24]	pixel	27.1	14.2	4.9	3.8	0.0	0.0	7.1	0.0	14.3	7.1	4.8
6 Grounding-DINO [29]	SED [41]	patch	42.7	15.2	<b>41.7</b>	26.9	<b>49.7</b>	0.0	0.0	53.7	<b>42.8</b>	25.7	27.1

## 6.2 Ablation on object detectors

To assess the influence of the open-set detector, we swap YOLO-World for Grounding-DINO inside MLFM (Table 5, rows 1 vs. 6). YOLO-World achieves slightly higher overall scores (+0.9 % SR, +1.7% SPL), yet Grounding-DINO proves stronger for specific attribute types: success rises by 3.8% for descriptions with no attributes, by 8.0% for *size*, and by 28.5% for *state*.

## 7 Limitations

The language in LangNav is still limited in several respects. First, the descriptions omit certain linguistic structures—coreference (e.g., “place *it* on the table”), negation (“a chair that is *not* black”), and anchor-based references (“the candle next to the *teacup*”). Second, only a small set of spatial relations is covered; cues such as “to the left of,” “behind,” or “under” are rare. Third, action directives are confined to simple verbs like *Go to* and *Find*, leaving out richer instruction patterns (e.g., “pick up,” “bring back,” or multi-step requests). Extending the dataset with these linguistic and spatial phenomena would broaden its coverage and support more advanced studies of language understanding in robotics and embodied AI.

## 8 Conclusion

We have introduced *LangNavBench*, a benchmark that probes semantic-navigation systems through rich natural-language goals. To support it we released *LangNav*, whose episodes feature sequences of three objects, manually verified descriptions, and per-instruction linguistic tags. We also proposed *MLFM*, a multi-layer mapping approach that preserves fine-grained visual detail and therefore improves language grounding. Systematic experiments and ablations show that MLFM surpasses state-of-the-art mapping baselines and that patch-level CLIP or BLIP-2 features, when stored across height slices, yield the best performance. Yet even with these gains, overall success rates remain well below 100 %, highlighting that LangNav is far from solved and offering ample headroom for new ideas in perception, memory, and language grounding. We also discussed the limitations of our dataset in terms of linguistic patterns and spatial relationships, which could enable future work in this direction. We hope that our findings in this paper provide useful insights into natural language understanding in embodied AI agents.

**Acknowledgement.** This work was funded in part by a CIFAR AI Chair, a Canada Research Chair, and NSERC Discovery grants. Infrastructure was supported by CFI JELF grants. TC was

supported by the PNRR project Future AI Research (FAIR - PE00000013), under the NRRP MUR program funded by the NextGenerationEU. We thank Jelin Raphael Akkara for sharing his viewpoint generation code to be used in this project. We also thank Francesco Taioli and Austin T. Wang for helpful discussions and feedback.

### Contributions.

**Sonia Raychaudhuri** created the LangNav dataset, implemented the MLFM codebase, re-implemented and integrated baseline methods, conducted all experiments reported in the paper, and contributed extensively to writing the paper.

**Enrico Cancelli** developed the initial codebase and performed preliminary experiments.

**Tommaso Campari** contributed to the refinement of ideas, coordinated the team, and was extensively involved in paper writing.

**Lamberto Ballan, Manolis Savva and Angel X. Chang** provided supervision, guidance throughout the project, and critical feedback on the manuscript.

### References

- [1] Peter Anderson, Angel Chang, Devendra Singh Chaplot, Alexey Dosovitskiy, Saurabh Gupta, Vladlen Koltun, Jana Kosecka, Jitendra Malik, Roozbeh Mottaghi, Manolis Savva, et al. On evaluation of embodied navigation agents. *arXiv preprint arXiv:1807.06757*, 2018. 1, 2, 4, 5
- [2] Peter Anderson, Qi Wu, Damien Teney, Jake Bruce, Mark Johnson, Niko Sünderhauf, Ian Reid, Stephen Gould, and Anton van den Hengel. Vision-and-language navigation: Interpreting visually-grounded navigation instructions in real environments. In *CVPR*, pages 3674–3683, 2018. 2
- [3] Dhruv Batra, Aaron Gokaslan, Aniruddha Kembhavi, Oleksandr Maksymets, Roozbeh Mottaghi, Manolis Savva, Alexander Toshev, and Erik Wijmans. ObjectNav revisited: On evaluation of embodied agents navigating to objects. *arXiv preprint arXiv:2006.13171*, 2020. 1, 2, 4, 14
- [4] Valts Blukis, Dipendra Misra, Ross A Knepper, and Yoav Artzi. Mapping navigation instructions to continuous control actions with position-visitation prediction. In *Conference on Robot Learning*, pages 505–518. PMLR, 2018. 6
- [5] Tom Brown, Benjamin Mann, Nick Ryder, Melanie Subbiah, Jared D Kaplan, Prafulla Dhariwal, Arvind Neelakantan, Pranav Shyam, Girish Sastry, Amanda Askell, et al. Language models are few-shot learners. *Advances in neural information processing systems*, 33:1877–1901, 2020. 4
- [6] Finn Lukas Busch, Timon Homberger, Jesús Ortega-Peimbert, Quantao Yang, and Olov Andersson. One map to find them all: Real-time open-vocabulary mapping for zero-shot multi-object navigation, 2024. URL <https://arxiv.org/abs/2409.11764>. 4, 5, 7
- [7] Matthew Chang, Theophile Gervet, Mukul Khanna, Sriram Yenamandra, Dhruv Shah, So Yeon Min, Kavitha Shah, Chris Paxton, Saurabh Gupta, Dhruv Batra, et al. Goat: Go to any thing. *arXiv preprint arXiv:2311.06430*, 2023. 17
- [8] Devendra Singh Chaplot, Dhiraj Prakashchand Gandhi, Abhinav Gupta, and Russ R Salakhutdinov. Object goal navigation using goal-oriented semantic exploration. In *NeurIPS*, volume 33, pages 4247–4258, 2020. 3
- [9] Shizhe Chen, Thomas Chabal, Ivan Laptev, and Cordelia Schmid. Object goal navigation with recursive implicit maps. *arXiv preprint arXiv:2308.05602*, 2023. 3
- [10] Tianheng Cheng, Lin Song, Yixiao Ge, Wenyu Liu, Xinggang Wang, and Ying Shan. Yolo-world: Real-time open-vocabulary object detection. In *Proceedings of the IEEE/CVF Conference on Computer Vision and Pattern Recognition*, pages 16901–16911, 2024. 6, 7, 9
- [11] Matt Deitke, Dhruv Batra, Yonatan Bisk, Tommaso Campari, Angel X Chang, Devendra Singh Chaplot, Changan Chen, Claudia Pérez D’Arpino, Kiana Ehsani, Ali Farhadi, et al. Retrospectives on the embodied AI workshop. *arXiv preprint arXiv:2210.06849*, 2022. 1
- [12] Shivam Duggal, Yushi Hu, Oscar Michel, Aniruddha Kembhavi, William T Freeman, Noah A Smith, Ranjay Krishna, Antonio Torralba, Ali Farhadi, and Wei-Chiu Ma. Eval3D: Interpretable and Fine-grained Evaluation for 3D Generation. *arXiv preprint arXiv:2504.18509*, 2025. 3

- [13] Samir Yitzhak Gadre, Mitchell Wortsman, Gabriel Ilharco, Ludwig Schmidt, and Shuran Song. Cows on pasture: Baselines and benchmarks for language-driven zero-shot object navigation. In *CVPR*, pages 23171–23181, 2023. 3
- [14] Theophile Gervet, Soumith Chintala, Dhruv Batra, Jitendra Malik, and Devendra Singh Chaplot. Navigating to objects in the real world. *Science Robotics*, 8(79):eadf6991, 2023. 3
- [15] Qiao Gu, Alihusein Kuwajerwala, Sacha Morin, Krishna Murthy Jatavallabhula, Bipasha Sen, Aditya Agarwal, Corban Rivera, William Paul, Kirsty Ellis, Rama Chellappa, Chuang Gan, Celso Miguel de Melo, Joshua B. Tenenbaum, Antonio Torralba, Florian Shkurti, and Liam Paull. Conceptgraphs: Open-vocabulary 3d scene graphs for perception and planning. *arXiv*, 2023. 3
- [16] Peter E Hart, Nils J Nilsson, and Bertram Raphael. A formal basis for the heuristic determination of minimum cost paths. *IEEE transactions on Systems Science and Cybernetics*, 4(2):100–107, 1968. 7
- [17] Chenguang Huang, Oier Mees, Andy Zeng, and Wolfram Burgard. Visual language maps for robot navigation. In *ICRA*, pages 10608–10615. IEEE, 2023. 3, 7
- [18] Christina Kassab, Sacha Morin, Martin Büchner, Matías Mattamala, Kumaraditya Gupta, Abhinav Valada, Liam Paull, and Maurice Fallon. OpenLex3D: A New Evaluation Benchmark for Open-Vocabulary 3D Scene Representations. *arXiv preprint arXiv:2503.19764*, 2025. 3
- [19] Mukul Khanna, Yongsan Mao, Hanxiao Jiang, Sanjay Haresh, Brennan Shacklett, Dhruv Batra, Alexander Clegg, Eric Undersander, Angel X Chang, and Manolis Savva. Habitat synthetic scenes dataset (hssd-200): An analysis of 3d scene scale and realism tradeoffs for objectgoal navigation. *arXiv preprint arXiv:2306.11290*, 2023. 14
- [20] Mukul Khanna\*, Yongsan Mao\*, Hanxiao Jiang, Sanjay Haresh, Brennan Shacklett, Dhruv Batra, Alexander Clegg, Eric Undersander, Angel X. Chang, and Manolis Savva. Habitat Synthetic Scenes Dataset (HSSD-200): An Analysis of 3D Scene Scale and Realism Tradeoffs for ObjectGoal Navigation. *arXiv preprint*, 2023. 1, 4
- [21] Mukul Khanna, Ram Ramrakhyia, Gunjan Chhablani, Sriram Yenamandra, Theophile Gervet, Matthew Chang, Zsolt Kira, Devendra Singh Chaplot, Dhruv Batra, and Roozbeh Mottaghi. GOAT-bench: A benchmark for multi-modal lifelong navigation. In *CVPR*, pages 16373–16383, 2024. 1, 2, 3, 4, 14, 17
- [22] Jacob Krantz, Stefan Lee, Jitendra Malik, Dhruv Batra, and Devendra Singh Chaplot. Instance-specific image goal navigation: Training embodied agents to find object instances. *arXiv preprint arXiv:2211.15876*, 2022. 1, 3
- [23] Alexander Ku, Peter Anderson, Roma Patel, Eugene Ie, and Jason Baldridge. Room-across-room: Multilingual vision-and-language navigation with dense spatiotemporal grounding. In *Proceedings of the 2020 Conference on Empirical Methods in Natural Language Processing (EMNLP)*, pages 4392–4412, 2020. 2
- [24] Boyi Li, Kilian Q. Weinberger, Serge J. Belongie, Vladlen Koltun, and René Ranftl. Language-driven semantic segmentation. *CoRR*, abs/2201.03546, 2022. 3, 7, 9
- [25] Junnan Li, Dongxu Li, Silvio Savarese, and Steven Hoi. BLIP-2: Bootstrapping language-image pre-training with frozen image encoders and large language models. In *International conference on machine learning*, pages 19730–19742. PMLR, 2023. 3, 7, 9, 14
- [26] Weijie Li, Xinhang Song, Yubing Bai, Sixian Zhang, and Shuqiang Jiang. Ion: Instance-level object navigation. In *Proceedings of the 29th ACM international conference on multimedia*, pages 4343–4352, 2021. 1, 3
- [27] Yifan Li, Yifan Du, Kun Zhou, Jinpeng Wang, Wayne Xin Zhao, and Ji-Rong Wen. Evaluating object hallucination in large vision-language models. *arXiv preprint arXiv:2305.10355*, 2023. 1
- [28] Jiachang Liu, Dinghan Shen, Yizhe Zhang, Bill Dolan, Lawrence Carin, and Weizhu Chen. What Makes Good In-Context Examples for GPT-3? *arXiv preprint arXiv:2101.06804*, 2021. 4
- [29] Shilong Liu, Zhaoyang Zeng, Tianhe Ren, Feng Li, Hao Zhang, Jie Yang, Qing Jiang, Chunyuan Li, Jianwei Yang, Hang Su, et al. Grounding dino: Marrying dino with grounded pre-training for open-set object detection. In *European Conference on Computer Vision*, pages 38–55. Springer, 2024. 9
- [30] Xiao Liu, Hao Yu, Hanchen Zhang, Yifan Xu, Xuanyu Lei, Hanyu Lai, Yu Gu, Hangliang Ding, Kaiwen Men, Kejuan Yang, et al. Agentbench: Evaluating llms as agents. *arXiv preprint arXiv:2308.03688*, 2023. 3

- [31] Dipendra Misra, Andrew Bennett, Valts Blukis, Eyvind Niklasson, Max Shatkhin, and Yoav Artzi. Mapping instructions to actions in 3D environments with visual goal prediction. In *EMNLP*, 2018. 6
- [32] OpenAI. GPT-4 technical report, 2023. 4
- [33] Alec Radford, Jong Wook Kim, Chris Hallacy, Aditya Ramesh, Gabriel Goh, Sandhini Agarwal, Girish Sastry, Amanda Askell, Pamela Mishkin, Jack Clark, et al. Learning transferable visual models from natural language supervision. In *International conference on machine learning*, pages 8748–8763. PMLR, 2021. 3, 9
- [34] Sonia Raychaudhuri, Tommaso Campari, Unnat Jain, Manolis Savva, and Angel X. Chang. MOPA: Modular Object Navigation with Pointgoal Agents. In *Proceedings of the IEEE/CVF Winter Conference on Applications of Computer Vision (WACV)*, pages 5763–5773, January 2024. 2, 4, 7
- [35] Sonia Raychaudhuri, Duy Ta, Katrina Ashton, Angel X. Chang, Jiuguang Wang, and Bernadette Bucher. Zero-shot Object-Centric Instruction Following: Integrating Foundation Models with Traditional Navigation, 2025. URL <https://arxiv.org/abs/2411.07848>. 2
- [36] Francesco Taioli, Edoardo Zorzi, Gianni Franchi, Alberto Castellini, Alessandro Farinelli, Marco Cristani, and Yiming Wang. Collaborative Instance Navigation: Leveraging Agent Self-Dialogue to Minimize User Input. *arXiv preprint arXiv:2412.01250*, 2024. 1, 3
- [37] Austin T. Wang, ZeMing Gong, and Angel X. Chang. ViGiL3D: A Linguistically Diverse Dataset for 3D Visual Grounding. *arXiv preprint*, 2024. doi: 10.48550/arxiv.2501.01366. 3, 4
- [38] Saim Wani, Shivansh Patel, Unnat Jain, Angel Chang, and Manolis Savva. MultiON: Benchmarking semantic map memory using multi-object navigation. *NeurIPS*, 33:9700–9712, 2020. 2, 4
- [39] Erik Wijmans, Abhishek Kadian, Ari Morcos, Stefan Lee, Irfan Essa, Devi Parikh, Manolis Savva, and Dhruv Batra. DD-PPO: Learning near-perfect pointgoal navigators from 2.5 billion frames. In *ICLR*, 2019. 7
- [40] Zhiyong Wu, Yaoxiang Wang, Jiacheng Ye, and Lingpeng Kong. Self-Adaptive In-Context Learning: An Information Compression Perspective for In-Context Example Selection and Ordering. In *The 61st Annual Meeting of the Association for Computational Linguistics (09/07/2023-14/07/2023, Toronto, Canada)*, 2023. 4
- [41] Bin Xie, Jiale Cao, Jin Xie, Fahad Shahbaz Khan, and Yanwei Pang. SED: A simple encoder-decoder for open-vocabulary semantic segmentation. In *CVPR*, pages 3426–3436, 2024. 6, 7, 8, 9
- [42] Karmesh Yadav, Santhosh Kumar Ramakrishnan, John Turner, Aaron Gokaslan, Oleksandr Maksymets, Rishabh Jain, Ram Ramrakhya, Angel X Chang, Alexander Clegg, Manolis Savva, Eric Undersander, Devendra Singh Chaplot, and Dhruv Batra. Habitat challenge 2022. <https://aihabitat.org/challenge/2022/>, 2022. 4
- [43] Karmesh Yadav, Ram Ramrakhya, Santhosh Kumar Ramakrishnan, Theo Gervet, John Turner, Aaron Gokaslan, Noah Maestre, Angel Xuan Chang, Dhruv Batra, Manolis Savva, et al. Habitat-Matterport 3D Semantics dataset. In *CVPR*, pages 4927–4936, 2023. 14
- [44] Sriram Yenamandra, Arun Ramachandran, Karmesh Yadav, Austin S Wang, Mukul Khanna, Theophile Gervet, Tsung-Yen Yang, Vidhi Jain, Alexander Clegg, John M Turner, et al. HomeRobot: Open-vocabulary mobile manipulation. In *CoRL*, pages 1975–2011. PMLR, 2023. 4
- [45] Naoki Yokoyama, Sehoon Ha, Dhruv Batra, Jiuguang Wang, and Bernadette Bucher. VLFM: Vision-language frontier maps for zero-shot semantic navigation. Workshop on Language and Robot Learning, CoRL 2023, 2023. Atlanta, GA, USA. 3, 7
- [46] Naoki Yokoyama, Ram Ramrakhya, Abhishek Das, Dhruv Batra, and Sehoon Ha. HM3D-OVON: A dataset and benchmark for open-vocabulary object goal navigation. *arXiv preprint arXiv:2409.14296*, 2024. 1, 2, 4
- [47] Jiazhao Zhang, Liu Dai, Fanpeng Meng, Qingnan Fan, Xuelin Chen, Kai Xu, and He Wang. 3D-aware object goal navigation via simultaneous exploration and identification. *arXiv preprint arXiv:2212.00338*, 2022. 3
- [48] Lingfeng Zhang, Xiaoshuai Hao, Qinwen Xu, Qiang Zhang, Xinyao Zhang, Pengwei Wang, Jing Zhang, Zhongyuan Wang, Shanghang Zhang, and Renjing Xu. Mapnav: A novel memory representation via annotated semantic maps for vlm-based vision-and-language navigation. *arXiv preprint arXiv:2502.13451*, 2025. 3

## A Supplementary Material

In this supplementary document we (i) present additional details of the LangNav corpus (Sec. A.1); (ii) describe the procedure used to generate and store episode viewpoints (Sec. A.2); (iii) report further ablations that quantify the contribution of each MLFM component (Sec. A.3); and (iv) evaluate MLFM on the Goat-Bench language-goal split (Sec. A.4).

### A.1 LangNav dataset

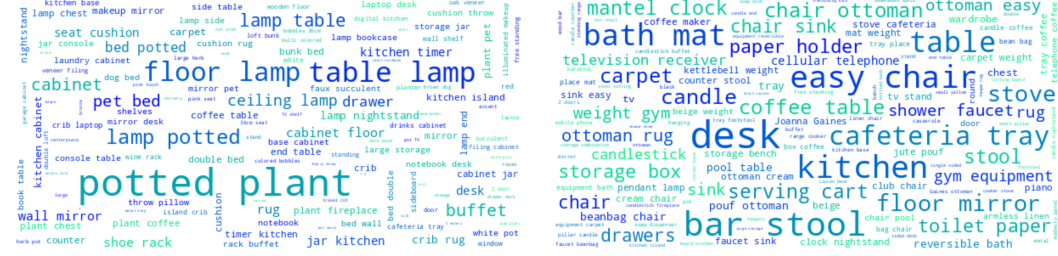


Figure 4: The left figure shows the objects that occur in the *test* split, while the right figure shows the objects occurring in the *val* split. Note that the objects in larger font appear more than the objects in smaller font.

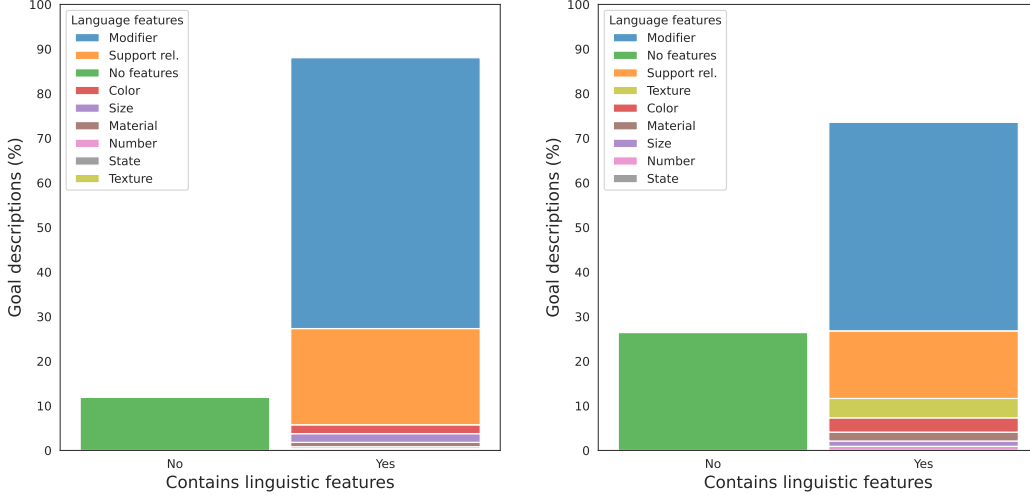


Figure 5: The left figure shows the percentage of goal descriptions for each linguistic feature in the *test* split, while the right figure shows the same in the *val* split.

**Understanding the dataset.** In this section, we visualize some statistics about our dataset by generating plots in order to gain insights into the dataset and understand the complexity of the task. We first highlight the most frequently occurring goal object categories in Fig. 4 for both the test (left) and the validation (right) splits. Note that the two sets are disjoint: the test split contains many *potted plants*, *table lamps*, and *floor lamps*, whereas the validation split contains many *easy chairs*, *desks* and *bar stools*. Moreover, LangNav also contains small objects such as *cellular telephone*, *notebook*, *clock*, *laptop* and so on. Next, we plot the distribution of goal descriptions over linguistic feature classes for the two splits in Fig. 5. The plot shows that LangNav includes more descriptions *with* explicit attributes than *without*. This highlights its usefulness as an evaluation dataset that focuses on natural language understanding and studying the ability of navigation models to ground various linguistic components. Among the linguistic features, the most frequent are *modifiers* (e.g., “easy



chair”) and *support relations* (e.g., “candle on night-stand”). We also plot the percentage of goal

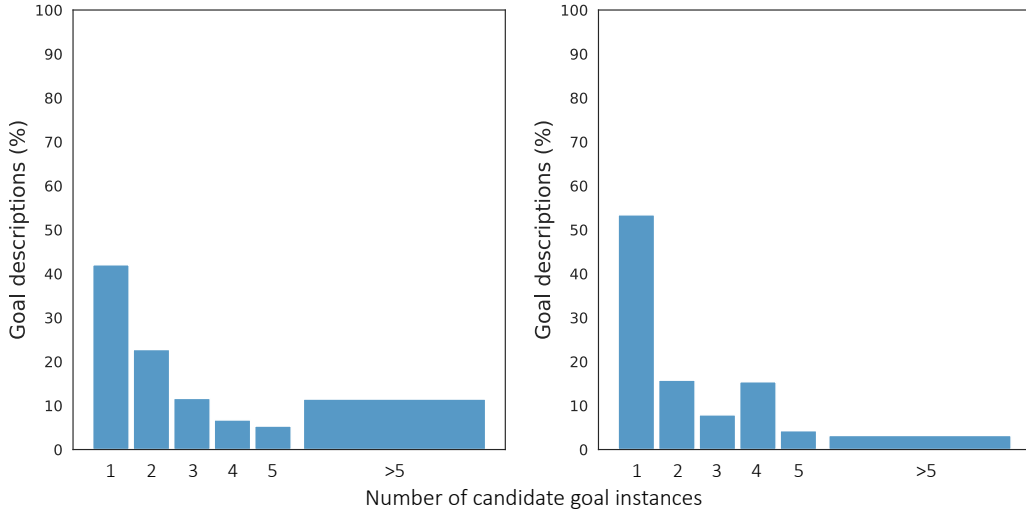


Figure 6: This plot shows that for majority of the episodes in both the splits (left is *test*, right is *val*), there exists only one candidate goal instance. Note that the x-axis plots the number of candidate goal instances while the y-axis plots the percentage of goal descriptions in the dataset.

descriptions against the number of candidate goal instances that exist in LangNav in Fig. 6. This plot shows that for the majority of the episodes in both the splits, there exists only one candidate goal instance. This indicates that our task is difficult since most of the time, the agent needs to find one very specific goal instance to make the navigation successful.

**Comparison with Goat-Bench.** Next we present an analysis on the Goat-Bench [21] dataset, focusing on their language goals, where the goals are specified using detailed descriptions. As noted in the main paper, the language-goal descriptions in Goat-Bench often inherit errors from the vision-language model BLIP-2 [25], which extracts object attributes from the image of each target. Fig. 7 illustrates five recurring issues. The *partial match* errors are where the instruction captures only some of the target’s attributes. The *hallucination* errors arise where BLIP-2 hallucinates attributes that are absent from the scene. The *mesh artefact* errors are those where the artefacts from the scene meshes influence BLIP-2’s ability to extract attributes. In HM3D-Sem [43] scenes, incomplete geometry (e.g., a missing refrigerator door) or irregular meshes can obscure or distort objects, causing BLIP-2 to generate spurious details such as non-existent “shards of glass”. The *reference to object bounding box* error occurs when the goal descriptions contain references to object bounding box, which the agent might not have access to during navigation (e.g. ‘...region defined by the bathtub bounding box’). And the *spatial errors* occur when the spatial relationship is wrong between objects (e.g. ‘blanket near the bed on the left side’ when it is clearly towards the foot of the bed in the figure). To obtain a statistic on how often these five error types occur, we randomly sample 100 goals from Goat-Bench and manually inspect the descriptions along with the corresponding goal images. We found that only 33% of them were accurate whereas the rest had errors - 22% were hallucination errors, 7% were mesh artefact errors, 3% were partial match errors, 23% were spatial errors and 12% were due to reference to object bounding box or the image frame, totaling to 67% error. The most frequent error types were spatial errors and hallucination errors.

To eliminate these problems, LangNav is built entirely from the synthetic HSSD scenes [19], whose geometry is free of such artefacts. Goal descriptions are generated from HSSD’s ground-truth attributes, yielding error-free instructions (see Fig. 8).

## A.2 Viewpoint generation

Similar to the ObjectNav task [3], we store *viewpoints* or navigable positions around the goal object, such that navigating near to any of those will be considered successful. To generate candidate viewpoints around an object, we use depth observations together with the object’s 3-D position and

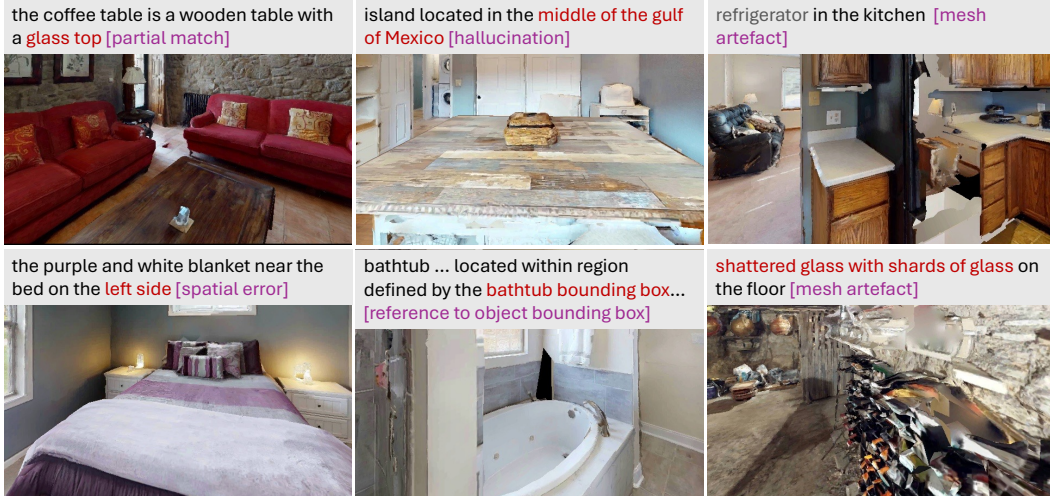


Figure 7: Language descriptions in Goat-Bench contain errors propagated from the BLIP-2 model. This figure shows examples for *partial match*, *hallucination*, *mesh artifact*, *spatial error* and *reference to object bounding box* errors.

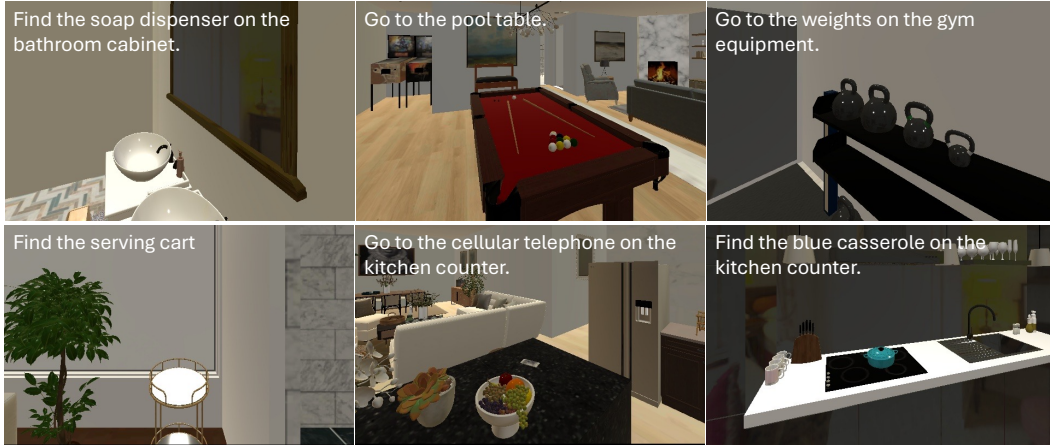


Figure 8: In LangNav, we use objects and attributes available in HSSD synthetic scenes, thus producing error free language descriptions.

dimensions to obtain viewpoints with a clear line of sight to the target object. First, we trace the object’s non-navigable boundary by sweeping a full  $360^\circ$  and recording every transition point from free space to obstacle. Around each boundary point we then place radial samples at uniform intervals out to 1.5 m. Each sample is accepted as a valid viewpoint only if it meets two criteria: the location is navigable, and—after orienting the agent toward the object—no intervening obstacle blocks the view. We describe the full algorithm below.

Table 6: Varying map resolution contributes towards MLFM’s performance.

cm per 2D grid cell	Num layers	SR↑	SPL↑	SR↑								
				no	color	size	texture	number	material	state	modifier	support
6	1	39.4	15.1	29.1	26.9	<b>41.7</b>	0.0	7.1	0.0	<b>57.1</b>	21.1	22.1
	2	42.9	16.3	36.9	<b>39.6</b>	32.9	0.0	<b>14.3</b>	<b>64.4</b>	14.3	<b>28.3</b>	26.0
	3	<b>43.6</b>	<b>16.9</b>	<b>37.9</b>	38.5	<b>41.7</b>	0.0	<b>14.3</b>	<b>64.4</b>	14.3	27.9	<b>27.3</b>
	4	43.0	15.3	20.3	38.1	<b>41.7</b>	0.0	0.0	9.7	14.3	16.0	17.4
	5	42.8	15.3	20.4	38.3	41.7	0.0	0.0	0.0	14.3	16.0	17.4
10	3	35.1	13.9	33.0	26.9	41.7	0.0	7.1	0.0	28.6	24.1	21.8

**Algorithm 1** generate\_view\_points**Require:** Input data  $obj\_pos, obj\_dims, dist_{bound}, radius_{bound}, dist_{vp}, radius_{vp}$ **Ensure:** Output *Viewpoints around the object*

```

1: Obtain boundary_points around the object
2: for  $\theta$  in  $(0, 2\pi)$  do
3:   Next equidistant  $pt_{bound} \leftarrow \text{Binary\_Search}(dist_{bound}, radius_{bound})$ 
4:   if  $pt_{bound}$  exists then
5:     Append  $pt_{bound}$  to boundary_points
6:   end if
7: end for
8: for  $pt_{bound}$  in boundary_pts do
9:   Compute equidistant  $radial\_pts \leftarrow f(radius_{vp}, dist_{vp})$ 
10:  for  $pt_{radial}$  in radial_pts do
11:    Skip if within previous  $pt_{bound}$  area
12:    Ensure  $pt_{radial}$  is navigable
13:    Face the Agent towards  $obj\_pos \leftarrow f(pt_{radial}, obj\_pos)$ 
14:    Compute corresponding pixel locations of  $obj\_dims$ 
15:    From Depth observation, obtain depth values at above pixel values
16:    if depth at  $px_{obj\_dims} >$  distance to  $obj\_dims$  then
17:      Append to view_pts
18:    end if
19:  end for
20: end for
21: return view_pts

```

**A.3 Ablations**

In this section, we report more ablations to determine how the different components contribute to MLFM’s performance. We ablate on grid resolution in Appendix A.3.1, followed by EAE percentage in Appendix A.3.2, the contribution of map and object detector in Appendix A.3.3 and finally the text-as-a-kernel querying mechanism in Appendix A.3.4.

**A.3.1 Effect of grid resolution and number of layers**

Tab. 6 reports an ablation on the two key map hyper-parameters: the number of height layers  $L$  and the  $(x, y)$  resolution of each slice. Success rises as  $L$  grows from one to three layers, but degrades when a fourth layer is added. Beyond three slices large objects become fragmented, making them harder to localise; we therefore set  $L = 3$  in all main experiments.

Keeping  $L$  fixed, performance improves when we refine the  $(x, y)$ -grid—i.e. when the centimetres-per-cell value decreases (rows 1 vs. 6). A finer resolution allows the map to preserve small objects geometry and thus boosts the agent’s success rate.

**A.3.2 Effect of explore-and-exploit (EAE) percentage**

Tab. 7 varies the share of the episode spent to Explore-and-Exploit (EAE) versus Exploit-only (E). Overall performance peaks when the agent spends the first 40% of its time budget in EAE and the

Table 7: Performance as we vary the percentage of time spent in Explore-and-Exploit (EAE). The remaining time is spent in Exploit-only.

EAE (%)	SR↑	SPL↑	SR↑									Error↓		
			no	color	size	texture	number	material	state	modifier	support	Wrong detection	Wrong goal on map	OOT
20	<b>43.6</b>	16.3	37.8	<b>38.5</b>	41.0	0.0	<b>14.3</b>	59.0	<b>14.3</b>	<b>27.9</b>	27.0	<b>25.1</b>	26.0	<b>48.9</b>
40	<b>43.6</b>	<b>16.9</b>	<b>37.9</b>	<b>38.5</b>	<b>41.7</b>	0.0	<b>14.3</b>	<b>64.4</b>	<b>14.3</b>	<b>27.9</b>	<b>27.3</b>	31.7	17.1	51.2
60	43.0	15.1	13.9	32.9	39.2	0.0	14.3	40.3	14.3	20.3	27.3	28.7	15.5	55.8
80	39.7	11.6	13.6	29.4	31.1	0.0	0.0	31.7	0.0	17.7	22.0	28.5	<b>8.2</b>	63.3

remaining 60% in E: both *Success Rate (SR)* and *Success weighted by Path Length (SPL)* achieve their highest values under this 40:60 split.

The table also reports the error composition. As the EAE portion grows, the *wrong-goal-on-map* rate declines, indicating that extended exploration yields a more accurate map. However, longer exploration leaves less budget for exploitation, so *out-of-time* failures increase once the EAE share exceeds 40%.

### A.3.3 Role of map and object detector in MLFM

Table 8: Role of map and object detector in MLFM.

Map	Object detector	SR↑	SPL↑	SR↑								
				no	color	size	texture	number	material	state	modifier	support
✓	×	43.0	16.1	<b>42.7</b>	30.7	<b>41.7</b>	0.0	<b>21.4</b>	61.1	14.3	<b>28.2</b>	27.3
×	✓	31.1	10.9	16.7	9.7	32.3	0.0	7.1	43.7	0.0	18.9	13.4
✓	✓	<b>43.6</b>	<b>16.9</b>	37.9	<b>38.5</b>	<b>41.7</b>	0.0	14.3	<b>64.4</b>	14.3	27.9	27.3

We next assess the individual contributions of the object detector and the multi-layer map. Tab. 8 compares three variants: map only, detector only, and the full system that combines both.

The *map-only* agent (row 1) matches the full model (row 3) on both *SR* and *SPL*, confirming that the multi-layer representation by itself is highly effective. By contrast, the *detector-only* variant (row 2) lags well behind, highlighting the importance of the spatial memory supplied by the map.

### A.3.4 Role of text-as-a-kernel querying technique

Table 9: This table shows that our text-as-a-kernel approach in MLFM benefits not only the overall performance, but also improves support relations.

text-as-a-kernel	SR↑	SPL↑	SR↑								
			no	color	size	texture	number	material	state	modifier	support
×	42.3	15.9	33.0	30.7	41.7	0.0	14.3	51.6	14.3	23.9	20.4
✓	<b>43.6</b>	<b>16.9</b>	<b>37.9</b>	<b>38.5</b>	41.7	0.0	14.3	<b>64.4</b>	14.3	<b>27.9</b>	<b>27.3</b>

We compare how the agent performance is affected when we query our multi-layer map without and with the text-as-a-kernel approach. It is evident from Tab. 9 that the text-as-a-kernel improves the support relationships by a large margin, thus leading to better overall performance.

## A.4 MLFM on Goat-Bench dataset

To demonstrate the effectiveness of our method MLFM, we perform an experiment on the language goals from the Goat-Bench [21] dataset.

**Task.** In the Goat-Bench task, an agent is required to sequentially navigate to multiple goals, described by the object category, a language description or an image of the object instance. In this paper, we focus only on the language goals where the goal object is described using a detailed description (e.g. ‘a black leather couch next to coffee table’).

**Baselines.** We compare our method MLFM to three baselines from the Goat-Bench paper, among which *Modular Goat* [7] is a zero-shot method, while the other two *RL Skill Chain* and *RL Monolithic*

are trained methods. In RL Skill Chain, individual navigation policies were trained on three different skills, ObjectNav, InstanceImageNav and LanguageNav, to tackle object category, image goal and language goals respectively. These policies are then combined using a third policy for high-level planner. On the other hand, RL Monolithic was trained end-to-end by using a multimodal goal encoder that encodes goals from different modalities into a common latent space. Our MLFM, being a zero-shot method is however comparable to the Modular Goat method, that builds a semantic map memory (containing object categories) as well as an instance-specific map memory (containing egocentric images and CLIP image features) during exploration.

**Results.** Tab. 10 shows that MLFM outperforms all baselines including the zero-shot method and the trained methods in both SR and SPL, on the language goals of Goat-Bench. MLFM improves the performance by +2.7% in SR and +5.3% in SPL.

Table 10: On the Goat-Bench dataset, MLFM outperforms the baselines on language goals.

Methods	trained	zero-shot	SR	SPL
RL Skill Chain	✓	×	16.3	7.4
RL Monolithic	✓	×	12.6	6.5
Modular Goat	×	✓	21.5	16.2
MLFM (Ours)	×	✓	24.2	21.5